J. Fluid Mech. (1990), *vol.* 212, *pp.* 663–684
Printed in Great Britain

Temperature overshoot due to quantum turbulence during the evolution of moderate heat pulses in He II

By W. FISZDON†, M. VON SCHWERDTNER, G. STAMM AND W. POPPE‡

Max Planck Institut für Strömungsforschung, Bunsenstrasse 10, D-3400, Göttingen, FRG

(Received 15 May 1989)

Transient heat transfer in liquid helium is investigated both experimentally and theoretically in plane and cylindrical geometry in the range of parameters where superfluid turbulence appears to be important. The influence of the main flow parameters – heat flux, pulse duration, and rest time – on the temperature evolution is reported. At high heat inputs the mutual friction force related to the superfluid vortex lines leads to the formation of a temperature overshoot behind the propagating second-sound wave and must be looked upon as a macroscopic effect of microscopic quantum turbulence. The experimental results can be reproduced by a theoretical model when the mutual interaction force is expressed in terms of the vortex line density (VLD), and the Vinen equation, extended to include spatial dependence, is taken into account for its temporal evolution. Fair quantitative agreement between experiment and theory is obtained if the ratio of the temperature overshoot and the shock-wave amplitude is below about 4. At stronger heat inputs the agreement is only qualitative.

1. Introduction

One of the many interesting and important macroscopic manifestations of quantum effects in superfluid helium is the existence of quantized vortices. The evolution of these vortices was noted by Feynman (1955) and formulated by Vinen (1957) and Schwarz (1978).

By analogy with classical fluids the vortex tangle when spread can be considered as quantum or superfluid turbulence. We shall not include a complete introduction to this problem in this paper, but only mention some recent and relevant references where this turbulence problem is discussed.

In his review Tough (1982) gives a full account of the results of the extensive research on quantum turbulence on stationary flow in tubes showing its influence on the character of the flow. Iznankin & Mezhov-Deglin's paper (1982) is concerned only with pulses of very short duration, below 10 μs. Donnelly & Swanson (1986) in their review on 'Quantum Turbulence' discuss very briefly the phenomenon of shock waves in superfluid helium. The pioneering, extensive, fundamental research on second-sound shock waves of the Graduate Aeronautical Laboratories, CalTech, are reviewed in the papers of Liepmann & Laguna (1984) and Liepmann & Torczynski (1986) where they point out that 'shock waves are a powerful probe of the physics,

† Permanent address: Polish Academy of Sciences and University of Warsaw.
‡ Temporarily at CNRS, LIMSI, Orsay, France.

thermodynamics and fluid mechanics of helium'. Torczynski's (1984) experiments on second-sound shock waves in rotating superfluid helium prove directly the influence of quantum vortices on the evolution of second-sound pulses. Turner (1983) was the first to note that at very high power inputs there exist large temperature overshoots 'beyond the shock limit' which he ascribed to the breakdown of superfluidity. An extensive set of experiments on the evolution of moderate plane and axisymmetric heat pulses in superfluid helium has been carried out at the Max-Planck-Institut für Strömungsforschung at Göttingen, to investigate the temperature variation in space and time and the relation that exists between the quantum turbulence level as measured by the vortex line density L, and the pulse parameters. Selected typical experimental findings are correlated with theoretical calculations based on a simple model deduced for the case of steady flow in tubes. Some previous results have been already published by Fiszdon & Schwerdtner (1989) and Schwerdtner, Stamm & Schmidt (1989).

In the present paper those results are extended and include the influence of pulse repetition on the overshoot in the plane and axisymmetric cases. The range of physical parameters, i.e. heat flux, heating time and temperature, is limited so as to avoid evaporation or phase transition to He I, which would unduly complicate this investigation.

First the experimental methodology and apparatus used will be briefly described. The simple theoretical model used to estimate the character of the pulse evolution will be given next, followed by a comparison of some experimental and theoretical results obtained. A possible physical picture of the evolution of the flow parameters will be provided at the end.

2. Experimental set-up

All experiments were performed at the helium laboratory of the Max-Planck-Institut at Göttingen. A ^{4}He bath cryostat of 7.2 cm diameter and 80 cm length, connected to a pump of 250 m^3/h displacement, capable of lowering the temperature down to 1.2 K, was used. The bath temperature could be adjusted by controlling the saturated vapour pressure using a Datametrics Barocel Pressure Sensor, an electronic manometer and a valve controller. The bath temperature was held constant within 0.05 mK of its set value.

The experimental cell, consisting of bottom and top plates made of stainless steel connected by four mounting rods, was fixed onto the framework of the experimental apparatus.

Two different flow channels were used as required by the geometry of the flow. For the plane symmetry case a rectangular channel of 6.76 cm^2 cross-section and 8 cm length, constructed of 0.3 cm thick lucite plates glued together, was used. The bottom end of the tube was closed by a quartz glass plate onto which a thin chromium film of about 120 Å and a resistance of $\approx 50\ \Omega$ was vacuum deposited to serve as a heater. To ensure a leaktight counterflow channel an indium seal was used between the channel socket and the heater substrate, and the leads were fed through holes drilled into the plate and soldered with indium (see figure 1).

For the axisymmetric geometry a cylindrical quartz tube of 0.5 cm diameter onto which a 1000 Å thick chromium layer was vacuum deposited was used as a heater. This cylinder was placed horizontally in the flow channel of 4.1 cm × 4.3 cm in cross-section. Two lucite plates were fixed at the ends of the quartz tube to form reflecting

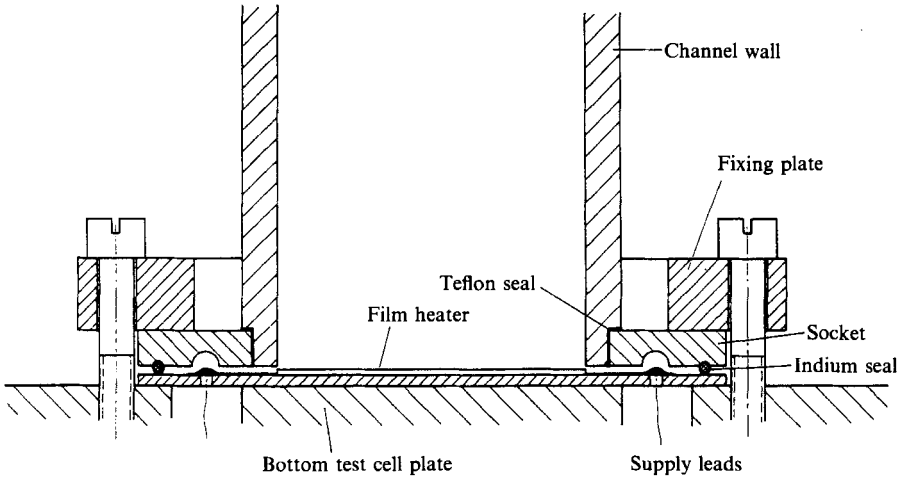

FIGURE 1. Lower part of the counterflow channel.

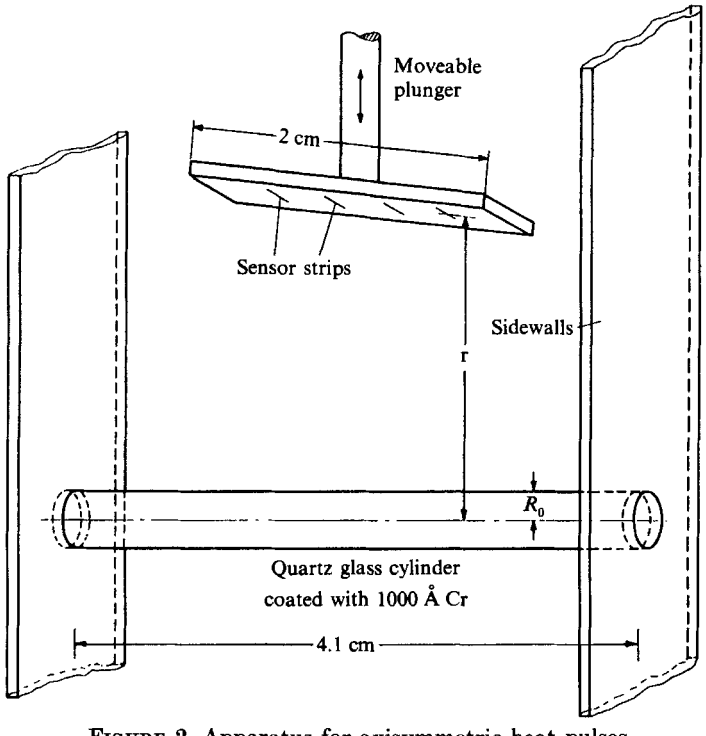

FIGURE 2. Apparatus for axisymmetric heat pulses.

walls, while the other walls of the channel were made non-reflective to eliminate disturbances from other parts of the channel (see figure 2).

In both cases the temperature probe was introduced into the channel from the upper end. The probe consists of a thin glass plate (2.4 cm × 4.0 cm × 0.01 cm) that is mounted in the streamwise direction in the channel. The sensor strip is a vacuum-deposited gold–tin film (20 μm wide, 1 mm long), located at the edge of the plate closest to the heater and connected to the leads of the amplifier by a conducting strip made of chromium, copper and gold (see figure 3). The sensor works as a sensitive

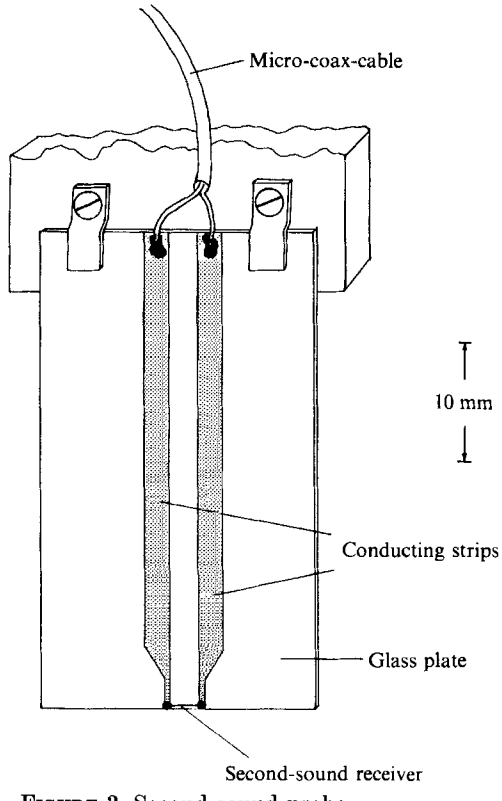

FIGURE 3. Second-sound probe.

superconducting bolometer near its critical temperature. By measuring the voltage drop along the sensor, operating typically at constant currents of 1 mA, very small temperature changes can be detected. Sensor sensitivities as high as 200 mV/K can be obtained. The composition of the sensor film was matched to the temperature of the helium bath. This type of temperature sensor was originally developed by the Liepmann group at CalTech and improved to be used without a magnetic field by Borner, Schmidt & Wagner (1979). The detectors were mounted on a movable plunger in the middle of the channel with the sensor strips adjusted horizontally. In the axisymmetric flow case they were parallel to the axis of the heater. The distance from the probes to the heater could be varied between 0 and 80 mm by means of a stepper motor outside the cryostat which is linked by a ferrofluid seal to a spindle on which the probe carrier is mounted. One step of the motor corresponds to a 2 μm sensor displacement.

The experiments were controlled by a suitably programmed microcomputer. First the computer evaluated the voltage corresponding to the desired heat flux of the second-sound wave, and transmitted it to a programmable power supply. A new measurement cycle began when the controlling quartz time base released a pulse. This pulse activated an electronic high-frequency switch coupling the power supply to the film heater. After the required heating time t_H, which had been selected using a digital delay unit (with an accuracy better than 0.5 μs), the stop pulse terminated the heating. When the wave reached the probe, the voltage drop along the sensor changed owing to the temperature rise and was amplified 1500 times by means of a wideband amplifier and recorded by a digital storing oscilloscope.

To obtain the real temperature value, the probes were first calibrated dynamically, i.e. short heat pulses (≈ 20 μs duration) were emitted and the amplitude of the received signal was measured as a function of the heat flux Q, from which the theoretical value of the second-sound amplitude, T_a, follows from the relation $T_a = A(T)\,Q$. For moderate heat pulses ($Q < 10$ W/cm^2) the coefficient $A(T) = 1/\rho c_2 c_p$ can be assumed constant at a given bath temperature. The calibration curve was obtained from a quadratic spline fit to the measured values.

The data processing was done by a microcomputer that stored the experimental parameters and the coefficients of the calibration curve, and collected the data that were recorded by the oscilloscope. A detailed description of the experimental set-up and procedure is given in Schwerdtner (1988) and Stamm (1988).

3. Simplified theoretical model

The basic equations describing the flow of He II result from the application of the set of conservation laws and reference frame invariance requirements adapted to the two-fluid model, as given for example in the monograph by Khalatnikov (1965) or by Putterman (1974). Because of the difficulty in obtaining exact analytical solutions to this set of nonlinear partial differential equations and the uncertainty concerning the numerical values of the hydrodynamic and thermodynamic parameters involved, an intermediate approach was attempted. To obtain a qualitative picture of the main flow features a simplified set of helium flow equations for a limited range of parameters was solved numerically on a personal computer.

Since the evolution of moderate second-sound heat pulses was of interest it was assumed that no displacement of the mass centre of gravity took place, so the following condition for the momentum was satisfied:

$$\rho \boldsymbol{v} = \rho_s \boldsymbol{v}_s + \rho_n \boldsymbol{v}_n = 0, \tag{3.1}$$

where ρ and $\boldsymbol{v}$ are the density and velocity, and the indices n, s denote the normal and superfluid components respectively.

By definition

$$\rho = \rho_n + \rho_s \tag{3.2}$$

and hence the velocities, following (3.1), can be expressed in terms of the counterflow velocity $\boldsymbol{w} = \boldsymbol{v}_n - \boldsymbol{v}_s$:

$$\boldsymbol{v}_n = \frac{\rho_s}{\rho}\boldsymbol{w}, \quad \boldsymbol{v}_s = -\frac{\rho_n}{\rho}\boldsymbol{w}. \tag{3.3}$$

The densities ρ, ρ_s, and ρ_n were assumed to be constant and the bulk viscosities were neglected.

Using as dependent variables the temperature T and the counterflow velocity $\boldsymbol{w}$ the set of conservation equations is reduced to the following two equations:

$$\frac{\partial \boldsymbol{w}}{\partial t} + \frac{\rho_s}{\rho}((\boldsymbol{w}\nabla)\,\boldsymbol{w} + (\nabla\cdot\boldsymbol{w})\,\boldsymbol{w} + \tfrac{1}{2}\nabla(\boldsymbol{w}\cdot\boldsymbol{w})) + \frac{s\rho}{\rho_n}\nabla T = \frac{\rho_s}{\rho\rho_n}(\eta\Delta\boldsymbol{w}), \tag{3.4}$$

$$\frac{\partial T}{\partial t} + \frac{\rho_s}{\rho}\boldsymbol{w}\cdot\nabla T + \frac{T s_0 \rho_s}{c_p \rho}\nabla\cdot\boldsymbol{w} = \frac{k}{\rho c_p}\Delta T, \tag{3.5}$$

where η is the shear-viscosity coefficient, c_p is the specific heat and k the coefficient of thermal conductivity.

The above basic equations (3.4) and (3.5) do not include possible effects due to superfluid vorticity and the additional forces due to the resulting interaction between

the normal and the superfluid component. However, because of the generated shock waves, rather strong perturbations of the equilibrium state were expected. So, unlike in the case of very slowly rotating fluids, it seems reasonable to assume that the superfluid vortices will develop into a vortex tangle and we shall be in the state of 'hopefully' homogeneous quantum turbulence. We shall assume that the phenomenological model of Gorter & Mellink (1949), although deduced for the case of steady flow in tubes, is also relevant in our case. Hence to account for quantum turbulence a term corresponding to the mutual interaction force, $-A\rho w^2 \boldsymbol{w}$, must be added on the right-hand side of (3.4), and a term corresponding to the energy dissipation, $(\rho_s \rho_n / \rho c_p) A w^4$, on the right-hand side of (3.5), where A is the so-called Gorter–Mellink coefficient and $w = |\boldsymbol{w}|$.

Vinen has shown that this coefficient A is related to the vortex line density L, which is the total vortex line length per unit volume, given by the relation:

$$A = \frac{1}{3} \frac{\kappa B}{\rho w^2} L. \tag{3.6}$$

Hence the Gorter–Mellink terms can be estimated to be of the order of w and w^2. From dimensional and phenomenological considerations Vinen (1957) deduced and Schwarz (1989) confirmed by microscopic calculations of the evolution of quantum vortices that the development of the vortex line density can be described by the following relation:

$$\frac{\partial L}{\partial t} + \nabla \cdot (\boldsymbol{v}_L L) = \chi_1 \frac{B}{2} \frac{\rho_n}{\rho} |\boldsymbol{w}| L^{\frac{3}{2}} - \chi_2 \kappa L^2, \tag{3.7}$$

where the divergence term on the left-hand side was added following Nemirovskii & Lebedev (1983) to take into account the motion of the vortex tangle. In (3.7) χ_1 and χ_2 are the growth and decay coefficients given by Vinen (1957), and B is the friction parameter introduced by Khalatnikov (1965). $\kappa = h/m$ is the quantum of superfluid circulation.

The velocity $\boldsymbol{v}_L$ of the vortex tangle is not a well-known quantity. As stated by Donnelly & Swanson (1986) there exists no unanimity between different authors on its value. Wang, Swanson & Donnelly (1987) compare their findings with other known results and with the latest theoretical model of Schwarz (1988) and conclude that the average tangle velocity is that of the superfluid. Some experimental observations of Schwerdtner (1988) hinted that the vortex tangle drifts slowly in the direction of the shock-wave propagation. Thus two different cases were tried out in the numerical calculations: the simple case of very small constant drift velocity proportional to the second-sound velocity; and the relation of Ashton & Northby (1975) giving values for the vortex velocity in the direction of the normal-fluid flow close to the ones deduced from Schwarz's (1978) theoretical model:

$$|\boldsymbol{v}_L| = C L^{\frac{1}{2}} + \frac{\rho_n}{\rho} |\boldsymbol{w}|, \tag{3.8}$$

where $\boldsymbol{v}_s$ has been replaced by $\boldsymbol{w}$ according to (3.3). From Vinen's experimental values it turned out that $C = 2.4\kappa$ for flow in tubes and can be taken as constant. Let us note that B and χ_2 vary with temperature and χ_1 is approximately constant.

It should be noted that this phenomenological way of introducing turbulence effects is based primarily on stationary flow measurements in tubes and rotating cylinders and its relevance in the prediction of propagation of heat pulses so far is not confirmed.

For the formulation of the equations of the approximate model to be solved it was convenient to introduce the following primed non-dimensional variables:

$$\left.\begin{aligned} T &= T_0 + \frac{c_{20}^2}{s_0}\frac{\rho_n}{\rho}T', \quad \frac{\rho_s}{\rho} = \rho_s', \qquad t = \frac{x_u t'}{c_{20}}, \\ w &= c_{20}\, w', \qquad\qquad x = x_u x', \quad x_u = 1 \text{ cm}, \end{aligned}\right\} \tag{3.9}$$

where

$$c_{20}^2 = \frac{\rho_s}{\rho_n}\frac{s_0^2 T_0}{c_p} \tag{3.10}$$

is the second-sound velocity, and T_0 and s_0 are the initial temperature and entropy. It was expected that, for the range of parameters used, an adequate qualitative description of the flow will be obtained when keeping terms up to second order and Landau & Lifshitz's (1959) requirement concerning superfluid vorticity. Thus our basic set of equations (3.4), (3.5) and (3.7), up to second-order terms, becomes:

$$\frac{\partial w'}{\partial t'} + \rho_s'((w'\nabla')\,w' + (\nabla'\cdot w')\,w' + \tfrac{1}{2}\nabla'(w'\cdot w')) + \nabla' T' = \eta'\Delta' w' - b_1 L' w', \tag{3.11}$$

$$\frac{\partial T'}{\partial t'} + \nabla'\cdot w' + \rho_s'\, w'\cdot\nabla' T' + T'\rho_s'\frac{s_0}{c_p}\nabla'\cdot w' = k'\Delta' T' + b_2 L' w'^2, \tag{3.12}$$

$$\frac{\partial L'}{\partial t'} + \nabla'\cdot(L' v_L') = \chi_1'|w'|L'^{\frac{3}{2}} - \chi_2' L'^2, \tag{3.13}$$

where

$$\left.\begin{aligned} L' &= L x_u^2, \qquad k' = \frac{k}{c_{20}\, x_u \rho c_p}, \quad \eta' = \frac{\rho_s}{\rho\rho_n}\frac{1}{c_{20}\, x_u}\eta, \\ b_1 &= \tfrac{1}{3}\kappa\frac{B}{c_{20}\, x_u}, \quad \frac{b_2}{b_1} = \frac{s_0\rho_s}{c_p\rho}, \qquad v_L' = \frac{v_L}{c_{20}}, \\ \chi_1' &= \tfrac{1}{2}\chi_1\frac{\rho_n}{\rho}B, \quad \chi_2' = \frac{\chi_2}{c_{20}\, x_u}\kappa. \end{aligned}\right\} \tag{3.14}$$

The form of the above set of basic equations suggests that at shorter times, when the terms containing second-order derivatives on the right-hand sides of (3.11) and (3.12) can be neglected, the flow field is described by a set of hyperbolic nonlinear equations and will have in general three characteristics. Hence the vortex tangle drift will not necessarily have a purely diffusional character.

To solve the set of equations (3.11)–(3.13) for a given case it is necessary to formulate the initial and boundary conditions. It was assumed that initially for $t < 0$ the system is at rest and in equilibrium except for the existence of a certain level of vortex line density L_0, due to physical or mechanical external disturbances present as noted for example by Awschalom & Schwarz (1984).

As a pulse is switched on, a heat input Q is generated at the heated boundary at $x = x_0$, and the entropy generated is entrained with the normal velocity v_n. Using (3.3), the corresponding counterflow velocity is given by the relation:

$$\left.\begin{aligned} w_0(x = x_0, t) &= \frac{Q}{\rho_s s_0 T_0} \quad \text{for} \quad 0 \leqslant t \leqslant t_H, \\ w_0(x = x_0, t) &= 0 \qquad\quad \text{for} \quad t > t_H, \end{aligned}\right\} \tag{3.15}$$

where t_H is the heating time. On the grounds of symmetry it was assumed that the temperature satisfies the Neumann boundary condition at the heated boundary:

$$\frac{\partial T}{\partial x} = 0 \quad \text{at} \quad x = x_0. \tag{3.16}$$

The initial and boundary conditions for the vortex line density L_0 are the most uncertain ones, since the physics of generation of superfluid vortices is not really known. Indeed Vinen (1957) introduced an additional term into his vortex line density evolution equation (3.7) to account for some 'mechanism by which turbulence can be initiated'. Therefore it was assumed initially that $L = L_0$ at $x > x_0$, and we shall therefore try out two different boundary conditions:
(*a*) the Neumann boundary condition

$$\frac{\partial L}{\partial x} = 0 \quad \text{at} \quad x = x_0, \tag{3.17}$$

and (*b*) the Dirichlet boundary condition

$$\left.\begin{array}{ll} L = L_a & \text{at} \quad x = x_0 \quad \text{and} \quad 0 < t < t_a \leqslant t_H, \\ L = 0 & t > t_a, \end{array}\right\} \tag{3.18}$$

which corresponds to the generation of quantum turbulence at the heated surface. Some numerical experiments have shown that in this case a better correlation with the experimental results can be obtained. This could be interpreted as the generation of vortices during the switch-on period of the heater. A comparison with experimental results may hopefully indicate which boundary condition is the most useful one.

As the solution of the set of equations (3.11)–(3.13) on a personal computer created difficulties in finding a convergent stable numerical procedure, they were transformed to a one-dimensional divergence form:

$$\frac{\partial}{\partial t'}\begin{pmatrix} w' \\ T' - \gamma\tfrac{1}{2}w'^2 \\ L' \end{pmatrix} + \frac{\partial}{\partial x'}\begin{pmatrix} T' + \tfrac{3}{2}\rho_s' w'^2 \\ w' + \rho_s' \dfrac{s_0}{c_p} T' w' \\ L' v_L' \end{pmatrix}$$

$$= \begin{pmatrix} \eta' \Delta_j' w' - b_1 L' w' - j\rho_s' \dfrac{w'^2}{x} \\ k' \Delta_j' T' + \gamma\eta' w' \Delta_j' w' + (b_2 - \gamma b_1) L' w'^2 - j\left(\dfrac{w'}{x'} + \rho_s' \dfrac{s_0}{c_p} \dfrac{T' w'}{x'}\right) \\ \chi_1' w' L'^{\frac{3}{2}} - \chi_2' L'^2 - j \dfrac{L' v_L'}{x'} \end{pmatrix}, \tag{3.19}$$

where $j = 0, 1, 2$ respectively for the cases of plane, cylindrical and spherical symmetry,

$$\gamma = \rho_s' \left(1 - \frac{s_0}{c_p}\right),$$

and third-order terms have been neglected.

This set of equations was solved numerically using the Richtmyer two-step version of the Lax–Wendroff method for the solution of the non-homogeneous set of partial differential equations. Details of the numerical scheme used are given in Fiszdon, Piechna & Poppe (1988).

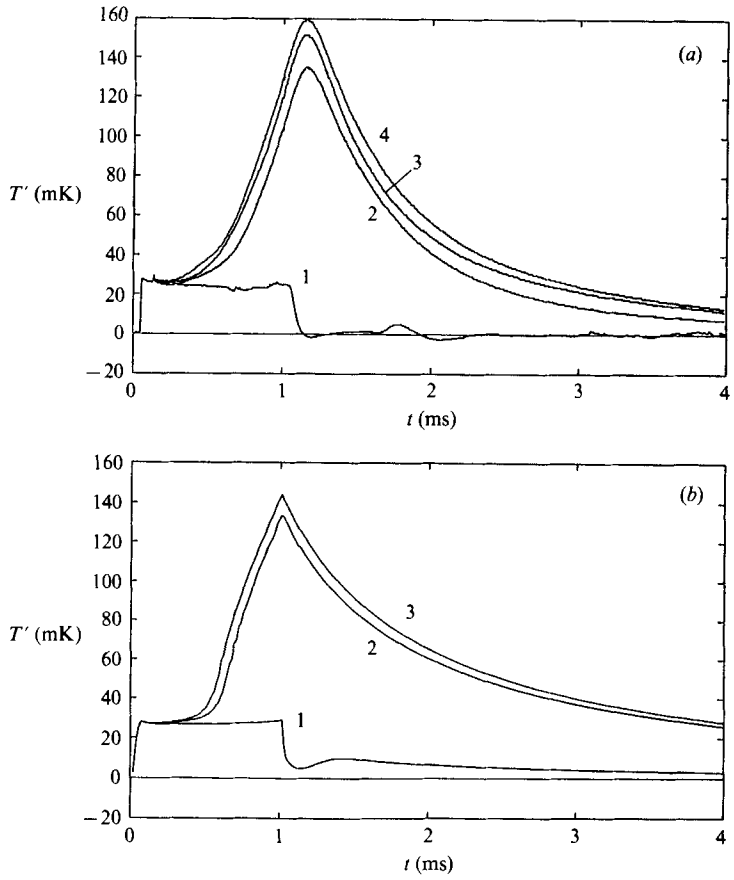

FIGURE 4. Sequence of temperature pulses at 1.4 K after a long resting time, obtained at 1 mm distance from the heater, in comparison with the calculated temperature evolution. The heat flux was 6 W/cm^2 and the pulse duration was 1 ms. (*a*) Experiment, (*b*) theory.

4. Experimental and theoretical observations

Experiments were done using heat pulses of 0.5 to 3 ms duration and power input intensity of 2 to 15 W/cm^2. The heating power rise time was of the order of 0.5 μs and therefore the pulse was considered as rectangular.

One of the main difficulties encountered was the repeatability of the results as influenced by the uncertainty of the initial vortex line density, which was affected by many external mechanical and radiation perturbations and is known to decay very slowly in superfluid helium. Since limited test time was available during each experimental session the selection of a test procedure which would yield consistent and repeatable data without unduly expanding the testing period was required. In his successive shock experiments Torczynski (1984) had observed that the first pulse, after a very long rest time, differed greatly from the following ones, which evolved on the background of a vortex field generated by the previous heat pulse and the perturbations they and other sources produced in the test section. This can be seen from the experimental measurements of the first few consecutive pulses of the temperature evolution in time at a distance of 1 mm from the heated plate on figure 4(*a*), and from the calculated similar temperature curves shown on figure 4(*b*). Fortunately, pulses repeated with a constant rest time, t_R, became practically

identical after a few cycles, the number of which depends on the initial conditions. Obviously each moderate heat pulse generates a certain amount of vorticity on the background vorticity field which remains. The generated vorticity decays slowly during the rest time before the next pulse is released. When the rest time is such that the vorticity field at the end of a cycle, consisting of a heating and a rest period, is the same as at its beginning, a stationary periodic state is reached. However, it should be noted that these observations although qualitatively confirmed by the numerical calculations made, using the approximate model described in §3, required greatly reduced rest times in the calculations when compared to the experimental rest times. This can be justified since the 'idealized' turbulence decay was calculated using the Vinen term without accounting for the finite dimensions of the test chamber or the influence of wave reflections from the walls and the free surface on the real turbulence field at large rest times.

The adopted test procedure was therefore to take the average of 5–10 short pulses at constant time intervals. The pulse times and bolometer positions were selected so as to avoid the effects due to wave reflections from the walls of the container or the free surface during the recording time. To compare with the experimental results the approximate theoretical solutions were obtained by solving numerically the set of equations (3.19) with all coefficients cited in §3. The only adjustable parameters used were the initial and boundary vortex line densities and the rest times which were adjusted so as to obtain a reasonable correlation with the experimental results. Test calculations done for a large range of pulse parameters, particularly for repeated pulses, have shown that at constant vortex line density (VLD) input rates at the heater, $\int_0^{t_H} L(x=0)\,\mathrm{d}t$, the Dirichlet boundary condition with the additional term allowing for the generation of quantum turbulence at the heated surface during a short time at the beginning of the pulse, appeared to be the most adaptable one to represent qualitatively the experimental results. With the Neumann boundary condition it was difficult to obtain the experimentally observed large temperature overshoots.

4.1. *Evolution of a plane temperature pulse*

Typical experimental temperature evolutions for the plane case at distances of 1, 2 and 5.4 mm from the heated surface are shown in figure 5(*a*). The pulse repetition rate is fixed at 5 s. The very large temperature overshoot close to the heater and the important temperature decay at a large distance away are the pronounced evident features of the pulse shapes. The corresponding calculated temperature variations, shown in figure 5(*b*), are qualitatively similar although there are some differences, for example in the position and sharpness of the maxima which could most likely be adjusted by varying the Gorter–Mellink coefficient or/and the parameters of the Vinen equation for the vortex line density and the other dissipation coefficients.

A fair comparison between the experimental observations and the numerical solutions of the approximate model was obtained. The influence of the main test parameters on the temperature overshoot was then examined. The temperature overshoot, T_{ov}, was defined as the ratio of the maximum temperature increase, appearing close to or beyond the heating time, to the temperature jump at the front of the shock wave. The main parameters that were controlled during the experiments at a fixed bath temperature were the heating time t_H, the power input Q, and the rest time between consecutive test pulses on each test run, t_R.

The variation of the temperature overshoot with the heating time at a distance of 5.4 mm from the heated surface is shown on figure 6 and the agreement with the

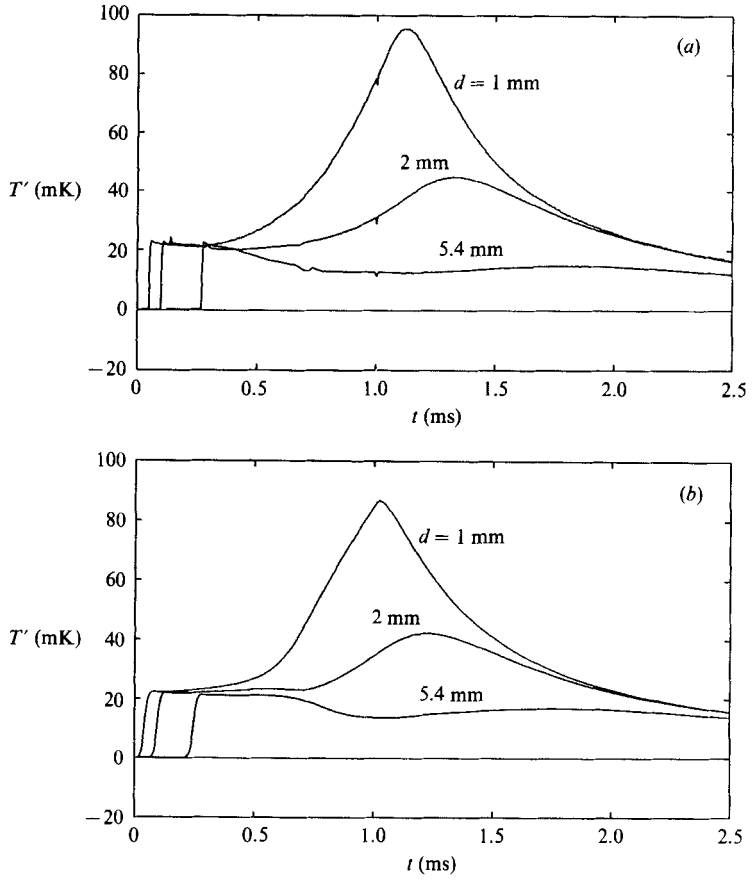

FIGURE 5. (*a*) Experimental and (*b*) theoretical temperature evolution at 1, 2, and 5.4 mm distance from the heater. The heat flux was 5 W/cm^2 and the pulse duration was 1 ms.

values calculated for $L_a = 3 \times 10^7/\text{cm}^2$ and $t_a = 0.025 t_H$, appears to be quite satisfactory. The evolution in time of the individual pulses seems to be closer to the experimental observations for $t_a \ll t_H$, and an appropriately larger value of L_a. The details of the measured temperature evolutions with time, at a distance of 5.4 mm from the heated surface for different heating times, can be seen in figure 7. It shows the smooth transition, after a gentle temperature decrease, to the overshoot temperature which increases with heating time. It should be noted that, at close distances to the heating surface, say of 1 mm, no temperature minimum was observed.

The dependence of the temperature overshoot on the power input at different distances from the heating surface is shown in the next figures. Figure 8 shows a comparison, for a bath temperature of 1.4 K, of the measured and calculated temperature overshoot variations for pulses of 1 ms duration with heat input. The main features are well correlated, but the differences in the amplitudes may be as large as 30%. Some experimental values of the variations of the temperature overshoot as a function of heat input at 1.4 K for heating times of 0.5 ms and 2 ms are shown in figure 9. The measured values of $T_{ov}(Q)$ are given in figure 10 for a bath temperature of 1.8 K, showing the same characteristic behaviour as those obtained at 1.4 K, in particular the non-monotonic variation of the overshoot for a heating

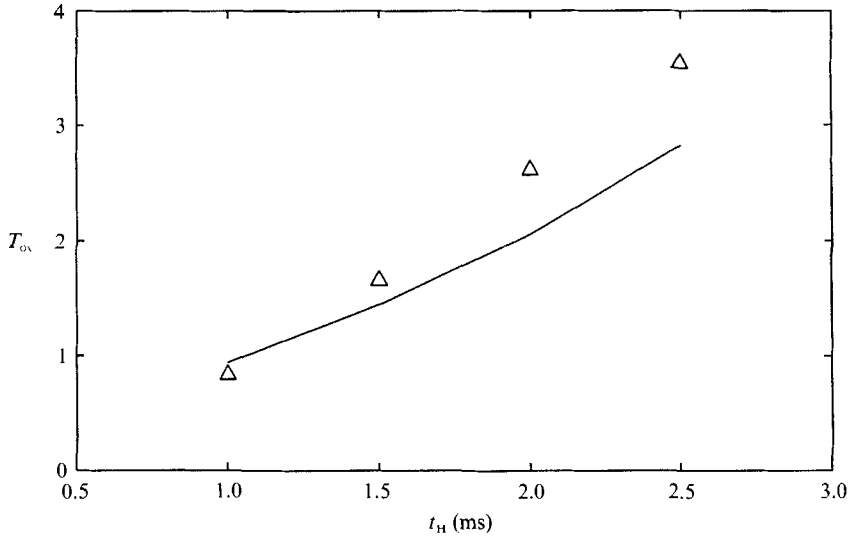

FIGURE 6. The temperature overshoot dependence on pulse duration for a heat flux of 6 W/cm² at 5.4 mm distance from the heater (△, experiment; solid line, theory).

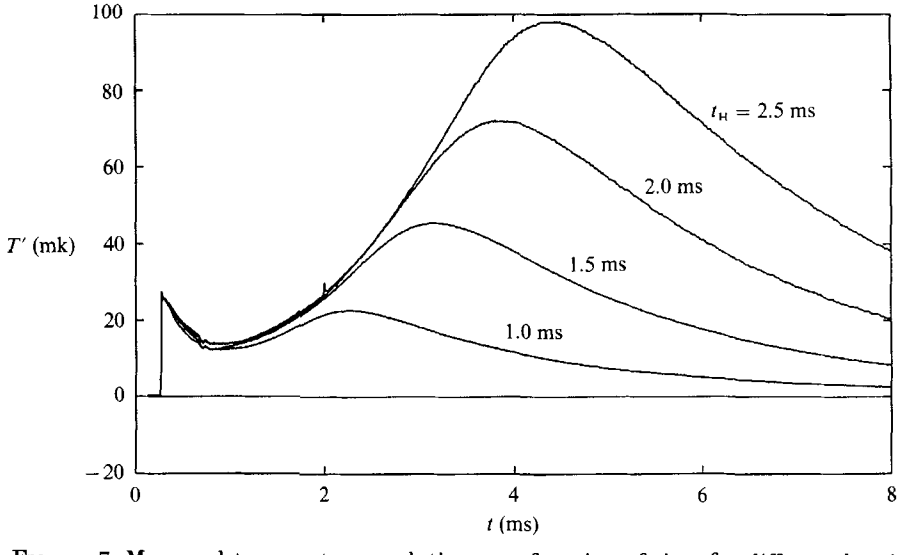

FIGURE 7. Measured temperature evolution as a function of time for different heating times t_H at a distance of 5.4 mm from the heater. The heat flux was 6 W/cm².

time of 1 ms and the decrease of dT_{ov}/dQ at the higher heater powers or temperature overshoots. The recorded evolution of the temperature increase above the bath temperature, T', as a function of time at a distance of 1 mm and 5.4 mm from the heated surface and different heat inputs are shown in figure 11. Clearly seen is the temperature maximum caused by the generation of quantum turbulence, which increases with the heating power, and its displacement away from the front of the second-sound shock wave with increasing distance from the heater. It is noted that the $T'(t, Q)$ curves at 5.4 mm are reminiscent of Turner's (1983) oscillograph record shown on his figure 5. Figure 12 shows the influence of the rest time between two

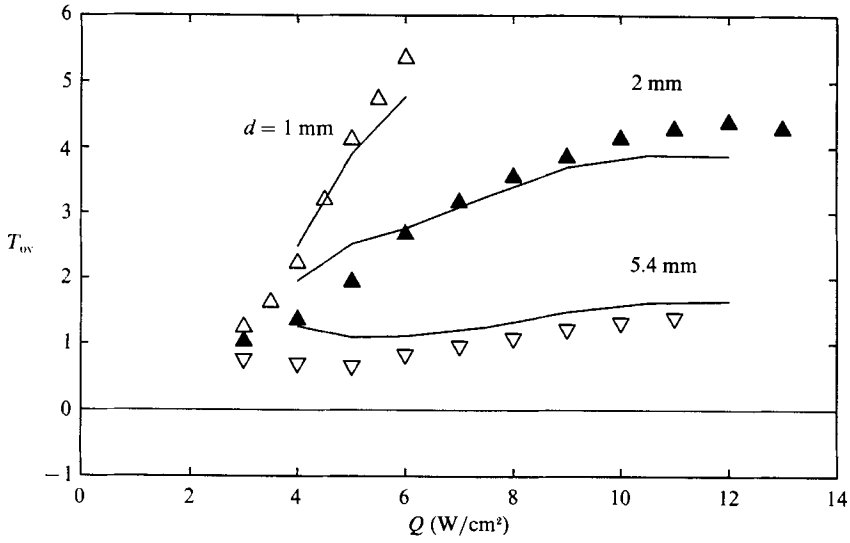

FIGURE 8. The temperature overshoot dependence on heat flux for various distances d from the heater. The pulse duration was 1 ms and the bath temperature was 1.4 K (△, ▲, ▽, experiment; solid line, theory).

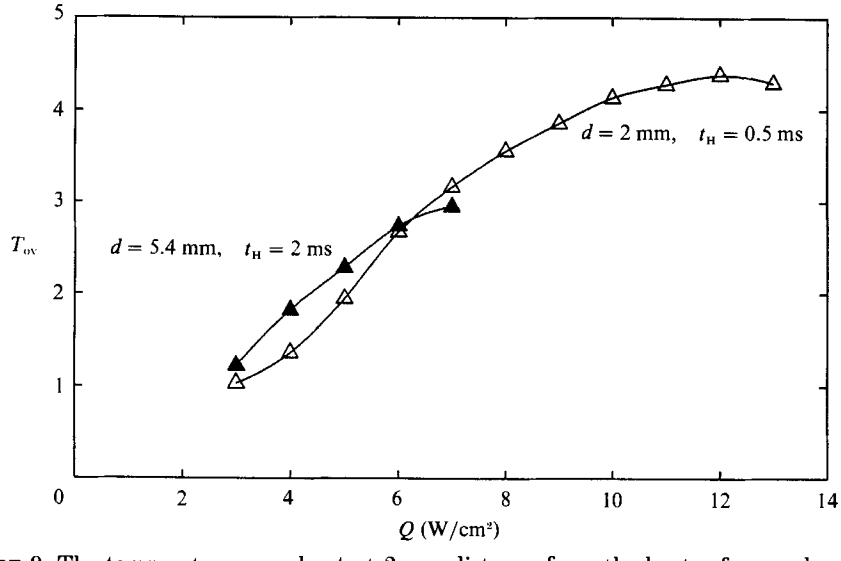

FIGURE 9. The temperature overshoot at 2 mm distance from the heater for a pulse duration t_H of 0.5 ms (△), and at 5.4 mm distance with t_H = 2 ms (▲). Lines are drawn to guide the eye.

consecutive heat pulses, t_R, on the shape of the temperature variation with time. The similarity of the above $T'(t, t_R)$-curve shapes with the $T'(t, Q)$-curves of figure 11 can be attributed to the quantum turbulence level. The quantum turbulence level is increased if the input is increased or if there is insufficient time between consecutive pulses for the turbulence to decay. The dependence of the overshoot maximum on the rest time is shown in figure 13.

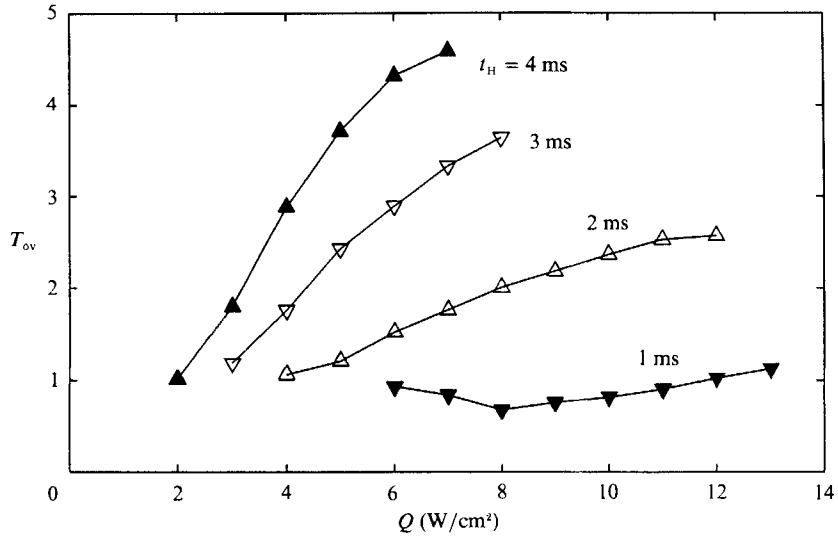

FIGURE 10. The temperature overshoot at 1.80 K bath temperature for various heating times t_H. The distance was 5.4 mm. Lines are drawn to guide the eye.

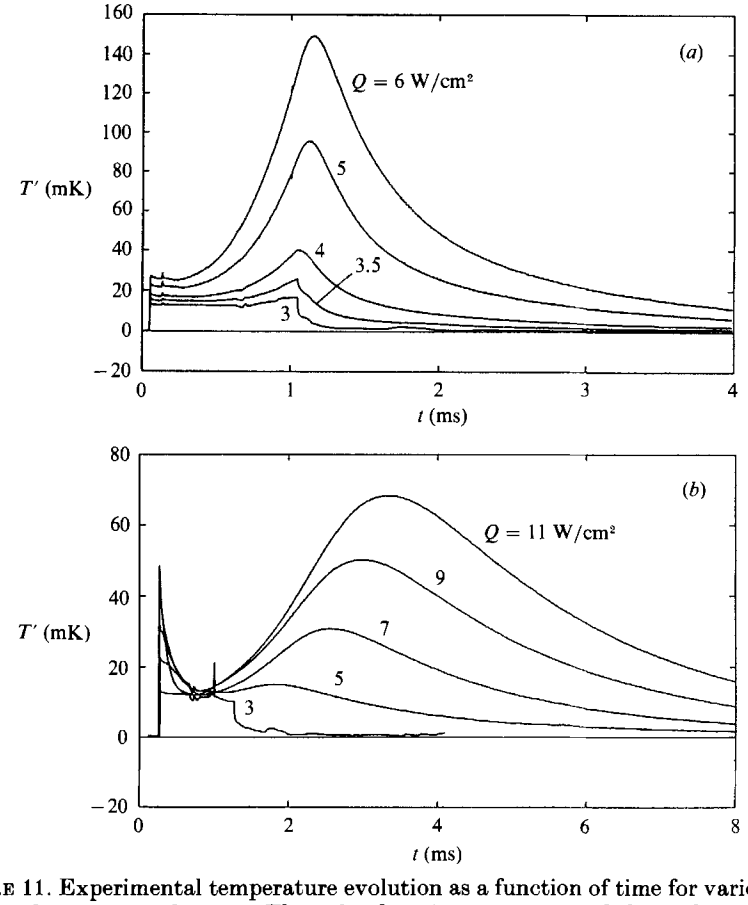

FIGURE 11. Experimental temperature evolution as a function of time for various heat fluxes at (*a*) 1 mm and (*b*) 5.4 mm distance. The pulse duration was 1 ms and the bath temperature was 1.4 K.

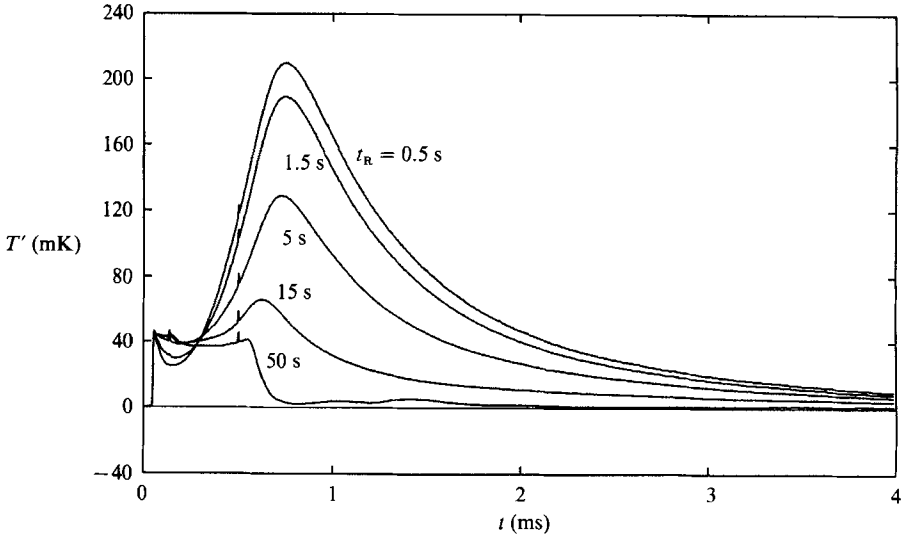

FIGURE 12. Experimental temperature evolution as a function of time for various pulse repetition times t_R at 1 mm distance. The heat flux was 10 W/cm² and the heating time was 0.5 ms.

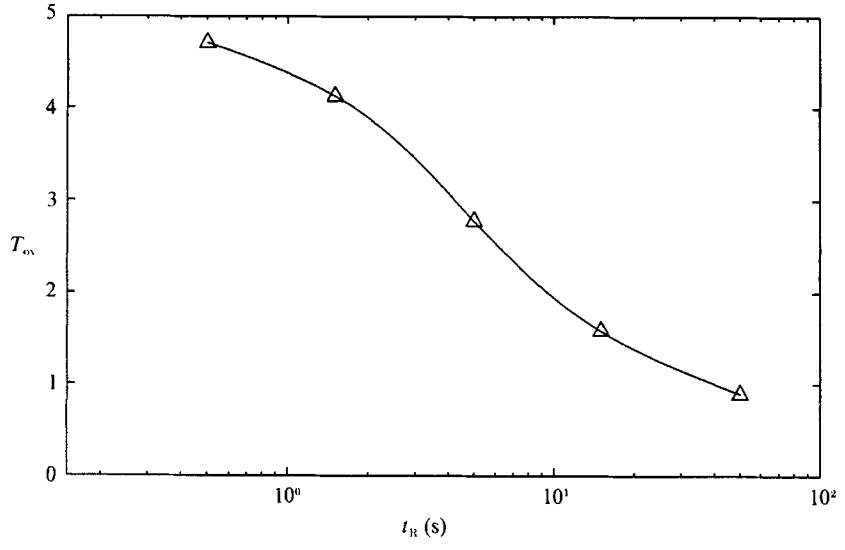

FIGURE 13. The dependence of the temperature overshoot on pulse repetition time. Parameters are as in figure 12. The line is drawn to guide the eye.

4.2. *Evolution of an axisymmetric temperature pulse*

Similarly to the plane case, the second-sound axisymmetric rectangular pulses were generated on the surface of a 0.5 cm diameter cylinder. All temperature measurements were taken before they could be affected by reflections from the walls of the test cell or free surface.

Typical shapes of the temperature evolution at distances of 1, 2 and 3 mm from the heated surface are shown in figure 14(*a*). If these results for the axisymmetric case are compared to those obtained in the plane case shown in figure 5 it can be seen that the general behaviour is similar in both cases.

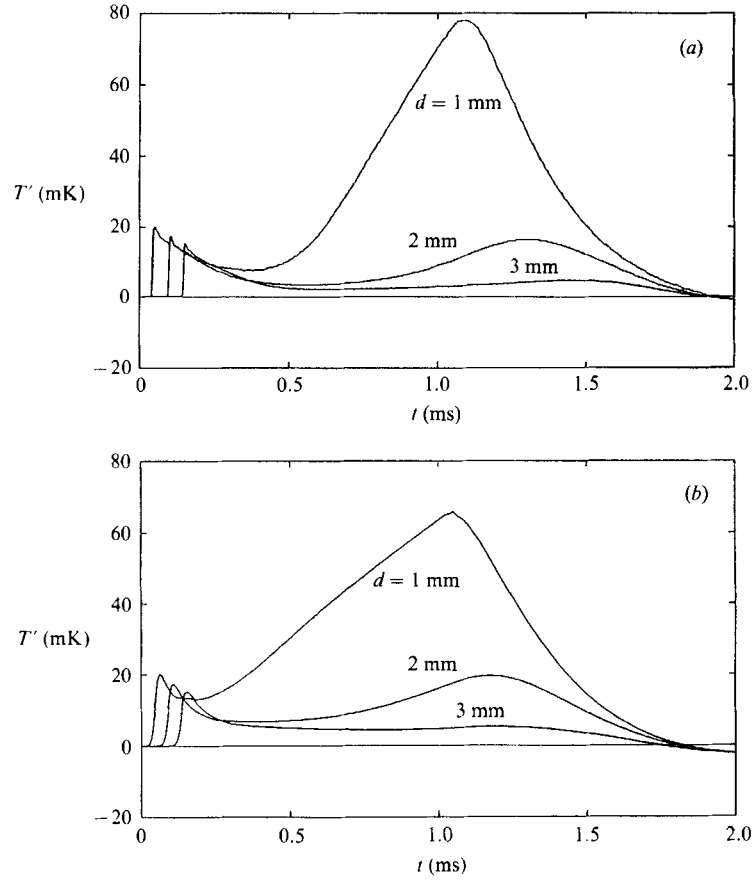

FIGURE 14. The evolution of temperature for the axisymmetric case for distances of 1, 2, and 3 mm from the heater. The bath temperature was 1.4 K, the heat flux 6 W/cm^2, the pulse duration 1 ms, and the pulse repetition time 0.5 s. (*a*) Experiment, (*b*) theory.

However, some particular features associated with the axisymmetric flow case are observed. First, there is a significant negative excursion of the temperature which is eventually overrun by the temperature overshoot. Secondly, steeper negative temperature gradients are experienced behind the wave front followed quickly by acute minima. Thirdly, the amplitudes of the temperature overshoot decrease more rapidly with increasing distance from the heater than in the plane case. The calculated values which correspond to the same case can be seen in figure 14(*b*) and show the same main qualitative features except for some slight differences in the local magnitudes.

The variation of the temperature overshoot as a function of heating time, at a distance of 1 mm from the heated surface is shown in figure 15. It is noted that the drastic change in the slope of the $T_{ov}(t_H)$ curve in figure 15 is very probably due to the start of evaporation at the heated surface. Boiling coincident with wave modification was observed also by Turner (1983). The power input variations for heating times of 0.5 ms and 1.0 ms and rest times of 0.1 s and 0.5 s are shown in figure 16. If these results are compared with the corresponding results for the plane case shown in figures 8 and 9 it is seen that the overshoot ratios are fairly close. This is reasonable to expect since the distance of $d = 1$ mm compared with the radius R_H of

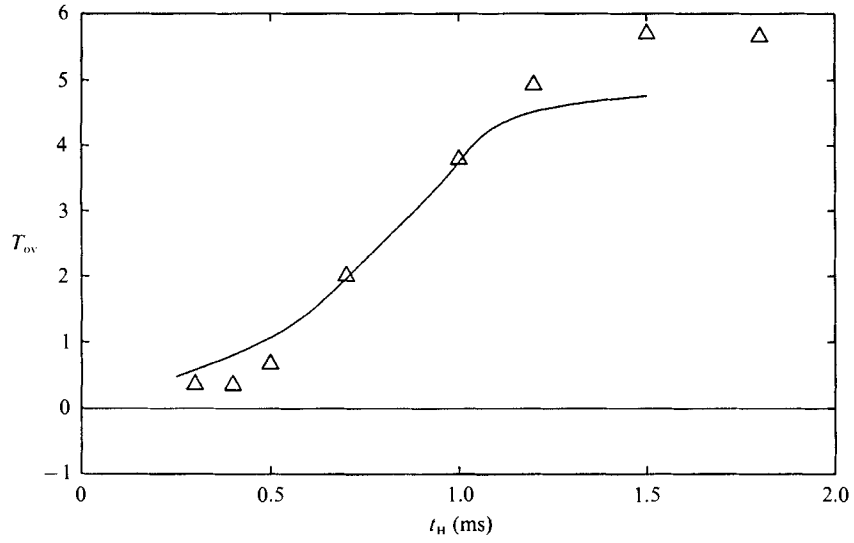

FIGURE 15. The temperature overshoot dependence on heating time at 1 mm distance for the case of axisymmetric heat pulses. The heat flux was 6 W/cm² and the rest time was 0.5 s (△, experiment; solid line, theory).

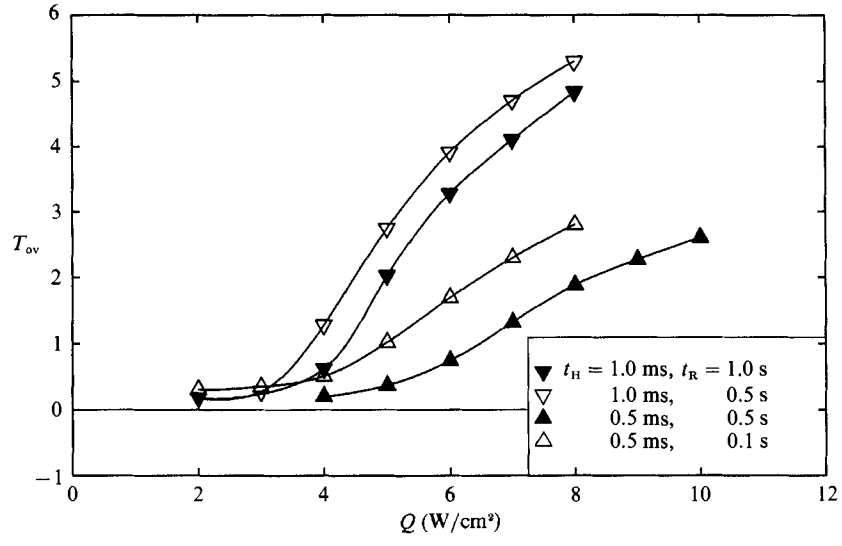

FIGURE 16. The temperature overshoot dependence on heat flux for various combinations of pulse duration and pulse repetition time at 1 mm distance from the heater for the axisymmetric case. Lines are drawn to guide the eye.

the heating cylinder ($d/R_H = 0.4$) is small, and hence the effects of the cylindrical geometry were not pronounced. The larger gradient of the curve in figure 15 when compared with that of the curve in figure 6 was not surprising since the distance from the heater was more than 5 times greater in the latter case.

The variation of the overshoot amplitude as a function of the rest time is shown in figure 17, where the significant dependence on the heating time is observed. The variation of the structure of the temperature pulse as a function of heat input and distance can be seen in figure 18. It is noted that at the closer distance of 1 mm, the

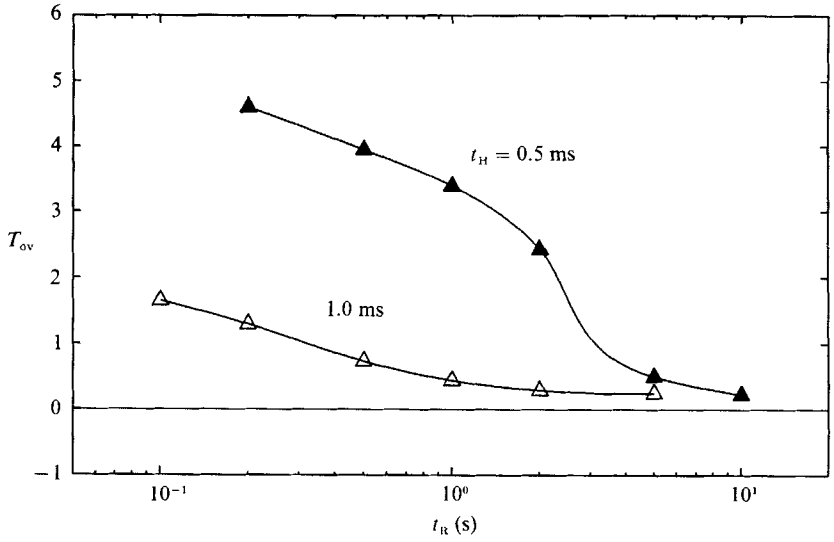

FIGURE 17. The axisymmetric temperature overshoot dependence on pulse repetition rate for two different pulse durations at 1 mm distance. The heat flux was 6 W/cm². Lines are drawn to guide the eye.

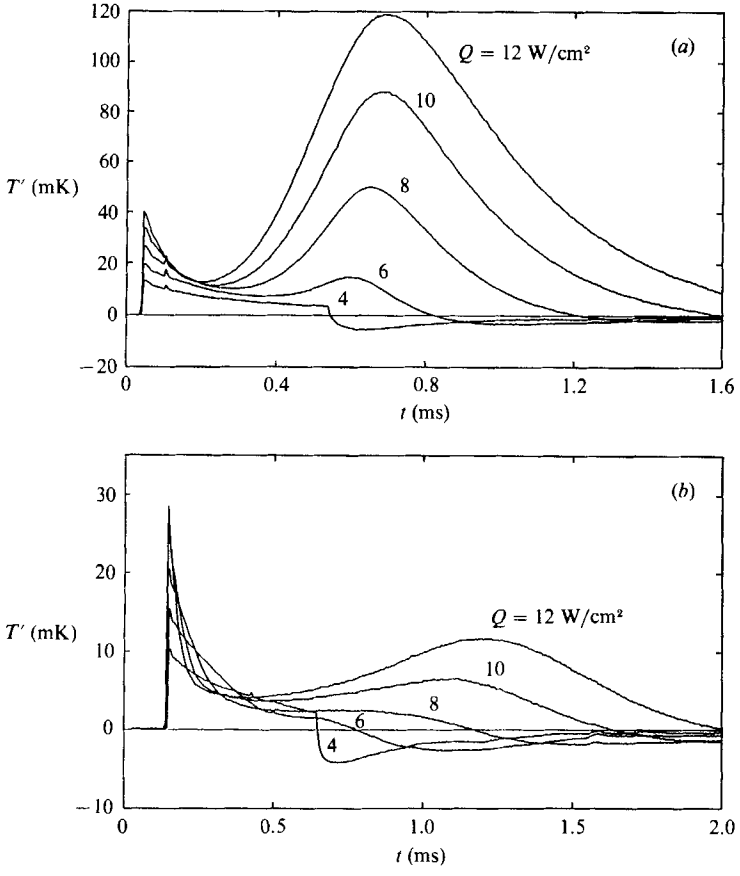

FIGURE 18. The temperature evolution as a function of time for various heat fluxes for the axisymmetric case for pulse duration of 0.5 ms, (*a*) at a distance of 1 mm and (*b*) at a distance of 3 mm.

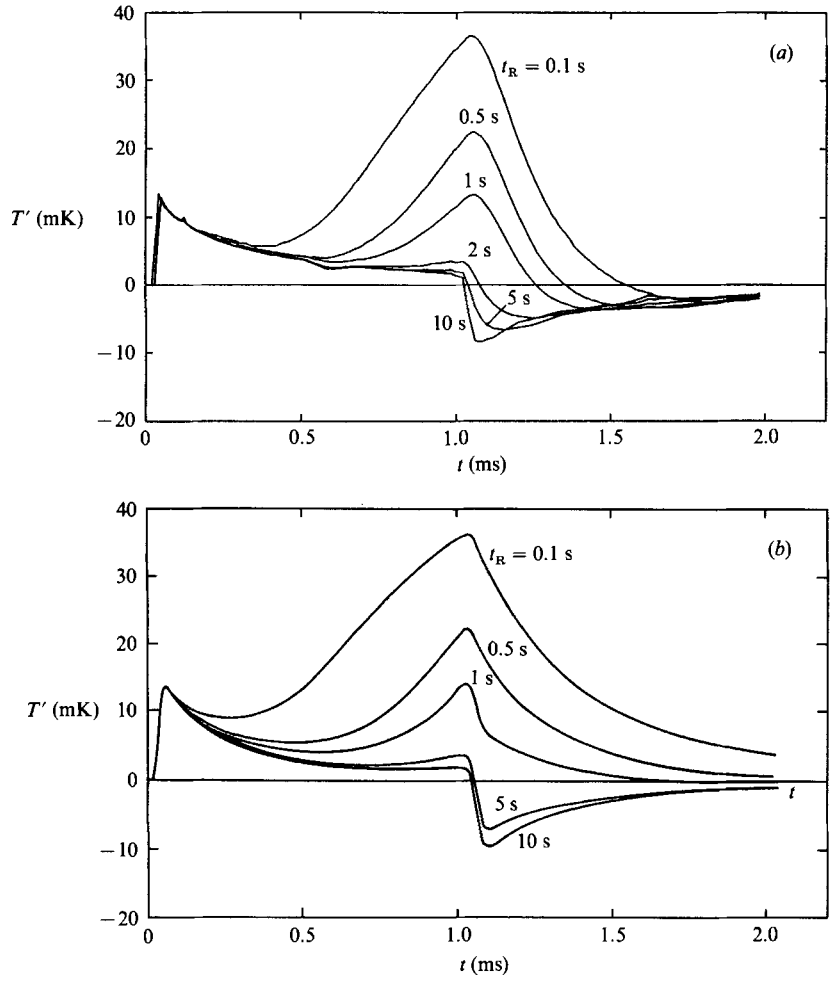

FIGURE 19. The effect of the pulse repetition rate on (*a*) the experimental and (*b*) the theoretical temperature evolution as a function of time at 1 mm distance from the heated surface in the axisymmetric case. The heat flux was 4 W/cm^2 and the pulse duration was 1 ms.

shape of the temperature curves remains similar except at the lowest heat input level where apparently no overshoot occurs since the turbulence level was negligible. At the larger distance the shape of the temperature curves appears to vary much more with larger overshoot amplitudes which completely disappears at the lower power inputs. As before, larger negative gradients exist directly behind the shock front.

In figure 19 the large influence of the rest time t_R on the (*a*) measured and (*b*) calculated temperature evolution is clearly illustrated. The qualitative agreement between the two sets of curves is reasonable.

5. Conclusions and remarks

The experimental results, supported by the theoretical calculations which were based on an approximate existing semi-phenomenological model, show the main characteristics of the evolution of finite-amplitude rectangular second-sound heat pulses. It is speculated that the appearance of temperature overshoots behind a

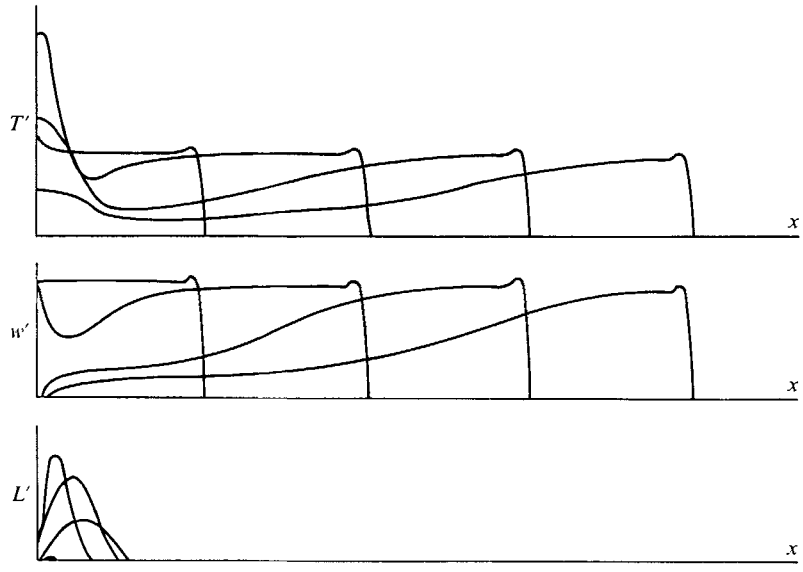

FIGURE 20. An example of the evolution of the counterflow velocity, the vortex line density, and temperature in space at successive time intervals during the passage of a plane second-sound pulse.

second-sound shock wave should be looked upon as a strong macroscopic manifestation of microscopic quantum effects rather than a breakdown of superfluidity. The superfluid quantized vortices which develop into a vortex tangle when averaged can be considered as quantum turbulence and serve as an intermediary agent which can strongly affect the flow field. It is noted that although the evolution of the quantum turbulence level as measured by the vortex line density (VLD) is approximately described by the Vinen (1957) model (see (3.7)), the initial production of quantum vorticity remains an open important question. The structural properties of the thin heating film and the initial rate of temperature increase may be significant in the production of quantum vorticity.

The temperature overshoots of single pulses which were released after a very long rest time strongly depend on the existing initial VLD. However, repeated pulses were practically independent of the initial VLD since they usually evolve in a strong vorticity field that they have produced, which has had insufficient time to decay.

The characteristic pattern of evolution of each pulse seems to be the following: The large counterflow velocity corresponding to a strong heat pulse leads to the growth of the initially present vortex lines, remaining from the preceding pulse. The superfluid vorticity evolves approximately in accordance with the Vinen model. The counterflow and hence the normal fluid velocity is strongly reduced by the growing vortex tangle close to the heater which results in heat accumulation and a large temperature increase in this region. This phenomenon can be clearly seen in figure 20 which shows an example of the temperature, counterflow velocity and VLD distribution in space at different times after a pulse was released. In all cases it was noted that immediately after initiating the heat pulse a distinct temperature and counterflow velocity propagating approximately with the second-sound velocity appeared. Far behind these waves the vorticity field followed as can be seen on the same figure.

The inclusion of the divergence term in the VLD equation (3.7) had only a small

influence on the position and value of the maximum of the temperature, and the justification of its inclusion in the proposed way remains an open question.

An enhanced understanding of the underlying physical processes and novel features of second-sound waves in superfluid helium have been brought about by the correlation of the experimental measurements and numerical results obtained in this investigation. The present results can be considered as an extension of Torczynski's (1984) research on successive shock experiments to the region closer to the heated surface and a larger range of parameters. Although the aim of the present work was to investigate the problem of temperature overshoot it allowed confirmation of the vortical character of the 'disturbances' produced near the heater by the shock wave and its qualitative description. However, even though the main experimental features are qualitatively in agreement with the theoretical predictions, the quantitative agreement was not quite satisfactory. This is primarily due to the inability to model theoretically the strong interaction between the velocity and vorticity fields in superfluid helium as well as the initial vorticity generation.

In spite of the qualitative agreement obtained, doubt remains as to whether the classical coefficients used in this investigation were the most appropriate ones. No attempt was made to vary them since there were already too many free parameters in the boundary and initial conditions to fit the experimental data which were limited only to the temperature evolution.

Future investigation which allows for simultaneous measurements related directly to the velocity and vorticity fields should provide a better opportunity to acquire more insight into the evolution of these fields. Hopefully this will help to improve our theoretical models and also lead to a better understanding of non-stationary processes in superfluid helium.

The authors would like to express their deep appreciation to Professor E.-A. Müller and D. W. Schmidt for their advice, interest and support of this research project. We would also like to express our special thanks to J. Pakleza, Z. Peradzynski and H. U. Vogel for the valuable discussions, suggestions and constant readiness to help during all stages of this research. Our thanks are also due to B. Noack for his help in improving the numerical program. The authors would also like to express their gratitude to the referees for their valuable remarks and suggestions.

The reported results form a part of the cooperative research program of the MPI für Strömungsforschung, Göttingen, FRG, and the CNRS, LIMSI, Orsay, France, and was supported in part by the Deutsche Forschungsgemeinschaft.

REFERENCES

Ashton, R. A. & Northby, J. A. 1975 Vortex velocity in turbulent He II counterflow. *Phys. Rev. Lett.* **35**, 1714–1717.

Awschalom, D. D. & Schwarz, K. W. 1984 Observation of remanent vortex line density in superfluid helium. *Phys. Rev. Lett.* **52**, 49–52.

Borner, H., Schmidt, D. W. & Wagner, W. J. 1979 A fast response superconducting thin-film probe for detection of second sound shock waves in superfluid helium. *Cryogenics* **19**, 89–92.

Donnelly, R. J. & Swanson, C. E. 1986 Quantum turbulence. *J. Fluid Mech.* **173**, 387–429.

Feynman, R. P. 1955 Application of quantum mechanics to liquid helium. In *Progress in Low Temperature Physics*, Vol 1 (ed. C. J. Gorter), pp. 17–53. North-Holland.

Fiszdon, W. F., Piechna, J. & Poppe, W. 1988 A qualitative numerical analysis of some features of propagation of counterflow temperature waves in superfluid helium. *MPI Strömungsforsch. Göttingen, Ber.* 9/1988.

FISZDON, W. F. & SCHWERDTNER, M. VON 1989 Influence of quantum turbulence on the evolution of moderate plane second-sound-heat-pulses in helium II. *J. Low Temp. Phys.* **75**, 253–267.

GORTER, C. J. & MELLINK, J. H. 1949 On the irreversible processes in liquid helium II. *Physica* **15**, 285–304.

IZNANKIN, A. YU. & MEZHOV-DEGLIN, L. P. 1983 Shock waves in liquid helium. *Zh. Eksp. Teor. Fiz.* **84**, pp. 1378–1390 (Soviet Phys. JETP **57**, 801–808).

KHALATNIKOV, I. M. 1965 *Introduction to the Theory of Superfluidity.* Benjamin.

LANDAU, L. D. & LIFSCHITZ, E. M. 1959 *Fluid Mechanics*, Ch. XVI. Pergamon.

LIEPMANN, H. W. & LAGUNA, G. A. 1984 Nonlinear interactions in the fluid mechanics of helium II. *Ann. Rev. Fluid Mech.* **16**, 139–177.

LIEPMANN, H. W. & TORCZYNSKI, J. R. 1986 Shock waves in helium at low temperatures. In *Proc. XV. Int. Symp. Shock Waves and Shock Tubes* (ed. D. Bershader *et al.*), pp. 87–96. Stanford University Press.

NEMIROVSKII, S. K. & LEBEDEV, V. V. 1983 The hydrodynamics of superfluid turbulence. *Zh. Eksp. Teor. Fiz.* **84**, 1729–1742 (*Soviet Phys. JETP* **57**, 1009–1016).

PUTTERMAN, S. J. 1974 *Superfluid Hydrodynamics.* North-Holland; Elsevier.

SCHWARZ, K. W. 1978 Turbulence in superfluid helium: steady homogeneous counterflow. *Phys. Rev.* B **18**, 245–262.

SCHWARZ, K. W. 1988 Three-dimensional vortex dynamics in superfluid ^{4}He: Homogeneous superfluid turbulence. *Phys. Rev.* B **38**, 2398–2417.

SCHWERDTNER, M. VON 1988 Experimentelle Untersuchung zum transkritischen Wärmetransport in He II. Ph.D. thesis, Mitt. MPI Strömungsforsch. Nr. 90, Göttingen.

SCHWERDTNER, M. VON, STAMM, G. & SCHMIDT, D. W. 1989 The evolution of superfluid vortex line density behind a second-sound pulse in He II. *Phys. Rev. Lett.* **63**, 39–42.

STAMM, G. 1988 Experimentelle Untersuchung zur zylindersymmetrischen Ausbreitung von Second-Sound-Stoßwellen in He II. M.S. thesis, MPI Strömungsforsch. Ber. 16/1988, Göttingen.

TORCZYNSKI, J. R. 1984 On the interaction of second sound shock waves and vorticity in superfluid helium. *Phys. Fluids* **27**, 2636–2644.

TOUGH, J. T. 1982 Superfluid turbulence. In *Progress in Low Temperature Physics*, Vol. 8 (ed. D. F. Brewer), Ch. 3, pp. 133–219. North-Holland.

TURNER, T. N. 1983 Using second sound shock waves to probe the intrinsic critical velocity of liquid helium II. *Phys. Fluids* **26**, 3227–3241.

VINEN, W. F. 1957 Mutual friction in a heat current in liquid helium II. III. Theory of mutual friction. *Proc. R. Soc. Lond.* A **242**, 493–515.

WANG, R. T., SWANSON, C. E. & DONNELLY, R. J. 1987 Anisotropy and drift of a vortex tangle in helium II. *Phys. Rev.* B **36**, 5240–5244.